Int. J. Electrochem. Sci., 16 **(2021)** 151046, doi: 10.20964/2021.01.74

International Journal of
ELECTROCHEMICAL
SCIENCE
www.electrochemsci.org

Anhydrous Proton Conduction of Soy Protein

Masanori Yamada[1,*], *Yuka Nagano*[1], *and Tetsuya Yamada*[2]

[1] Department of Chemistry, Faculty of Science, Okayama University of Science, Ridaicho, Kita-ku, Okayama 700-0005, Japan
[2] Research Faculty of Agriculture, Hokkaido University, Sapporo 060-8589, Japan
[*]E-mail: myamada@chem.ous.ac.jp

Received: 9 October 2020 / *Accepted:* 16 November 2020 / *Published:* 30 November 2020

Water-soluble soy protein contains a large amount of acidic amino acids, such as glutamic and aspartic acids. Since these acidic amino acids possess the –COOH group in their side chain, the water soluble soy protein acts as an acidic polymer. Therefore, we prepared a composite material by the mixing of acidic protonated soy protein (SPH) and a basic heterocyclic molecule, such as imidazole (Im). The SPH-Im composite materials showed a thermal stability at ≤130 °C by the acid-base interaction between the acidic –COOH group, related to the side chain of the acidic amino acids, and basic Im molecule. Additionally, the proton conductivity of the SPH-Im composite material increased with the mixing of the Im molecule and reached a maximum proton conductivity at R=0.2. This proton conductivity was 4.4×10^{-4} S cm^{-1} at 130 °C under flowing dry nitrogen. Furthermore, the E_a of the proton conduction in the SPH-Im composite material was 0.27 – 0.76 eV. These results suggested that the proton conductive mechanism in composite material was based on the anhydrous proton transfer from the –COOH group to the deprotonated –COO$^-$ group.

Keywords: Composite material, Soy protein, Anhydrous proton conduction, Polymer electrolyte, Acidic amino acid

1. INTRODUCTION

Soybean, one of the most familiar crops, has been cultivated and eaten around the world. In addition, since soybean contains approximately 20% fat by weight of the dry soybean [1,2], a large amount of soybeans has been used as a crop to obtain its oil for use as cooking oils, industrial oils, and chemical agents. As a result, the degreased soybean has been produced as a secondary product throughout the world. Although part of the degreased soybean, one of its secondary products, is used for the food of human consumption and livestock feed or fertilizer, a lot of the degreased soybeans is discarded as industrial waste [2]. Therefore, for utilization of the degreased soybeans, various materials, such as a drug delivery system [3], tissue engineering [4], and antimicrobial material [5], have been

reported. Recently, we also reported a novel bioplastic with a biodegradable property by using degreased soybeans [6]. However, these degreased soybeans have been utilized in only the biological- and environmental-fields, while the applications for electrochemical or optical devices are quite limited. In contrast, the soy protein (SP), which is obtained from the degreased soybean, contains various amino acids, such as aspartic acid (Asp), glutamic acid (Glu), glycine (Gly), alanine (Ala), valine (Val), leucine (Leu), lysine (Lys), and arginine (Arg) [7]. Especially, the water-soluble SP possesses a large amount of acidic amino acids, such as Glu and Asp. Therefore, the protonated SP (SPH), in which the alkaline metal ion in the water-soluble SP was changed to a proton, acts as an acidic polymer with the mobile proton. These acidic polymers with the mobile proton can be used as a proton conductor, actuator, or for electrochromism [8]. The proton conductor using a soy protein has not been reported to the best of our knowledge.

The anhydrous proton conductor has attracted attention as the important element of the polymer electrolyte membrane fuel cell (PEFC) operated at intermediate temperature (100 - 200 °C) or under anhydrous or extremely low humidity conditions [9,10]. Although the humidified Nafion® membrane, one of the most famous perfluorinated sulfonic acid membranes, has a high proton conductivity at <100°C (boiling point of water), this conductivity abruptly decreases at intermediate temperature or under anhydrous or extremely low humidity conditions [11]. This is because the proton conductive mechanism of the humidified Nafion® membrane is based on the vehicular mechanism, in which the proton transfers with the assistance of diffusible water molecules, and the water molecule in the membrane evaporates under these conditions [11]. Therefore, the proton transport under an anhydrous condition requires the non-vehicular mechanism, in which only the protons are mobile from the proton donor site to the proton acceptor site without diffusible water molecules [12-15]. In this case, the distance between the proton donor and proton acceptor is very important [12,13]. In contrast, the biopolymers, such as polysaccharides, proteins, and nucleic acids, possess various functional groups in the polymer chain and the distance between these groups are close [16,17]. Therefore, the soy protein, which acts as an acidic polymer, has the potential to be used as an anhydrous proton conductor.

In this study, we prepared the composite material by the mixing of the acidic protonated soy protein (SPH) and a basic heterocyclic molecule, such as imidazole (Im). The SPH-Im composite materials showed a thermal stability at ≤130°C by the acid-base interaction between the acidic –COOH group, related to the side chain of the acidic amino acids, and the basic Im molecule. In addition, the SPH-Im composite material indicated the proton conductivity of 4.4×10^{-4} S cm^{-1} at 130 °C under flowing dry nitrogen. Furthermore, the proton conductive mechanism depends on a non-vehicular mechanism, in which only protons are mobile from the proton donor site to the proton acceptor site without diffusible molecules.

2. EXPERIMENTAL

2.1. Materials.

Soy protein (SP) and imidazole (Im) were purchased from Fujifilm Wako Pure Chemical Industries, Ltd., Osaka, Japan. The purification of SP was performed by the following procedure: the SP

powder was stirred in methanol for 1 hour to remove the organic solvent-soluble components, the residue separated by filtration, then dried at room temperature overnight. The residue was dissolved in water, then the water-insoluble component was removed by centrifugation. The water-soluble SP component-containing aqueous solution was freeze-dried for 2 days.

The strongly acidic ion-exchange resin Amberlite IR120(H) was obtained from Supelco, Bellefonte, PA. The solvents were used an analytical grade in all the experiments described. Ultra-pure water (Merck KGaA, Darmstadt, Germany) was used in this experiment.

2.2. Preparation of the SPH-Im composite materials

In general, the SP material contains the alkaline metal ions, such as sodium and potassium ions. Therefore, the metal ion in the SP material was changed to H^+ by an ion exchange column using a strongly acidic ion exchange resin [18]. The ion exchange of SP was confirmed by the pH measurement. The resulting aqueous solution of the protonated SP (SPH) was freeze-dried for 2 days and used in the experiments.

The SPH-Im composite materials were prepared by the following procedures: the SPH (50 mg/ml) and Im molecule were dissolved in water. The SPH-Im solution (50 or 100 μl) was cast onto a Teflon® plate, dried at 60°C for 1 hour, then heated at 100°C for 30 min. The dried-membrane or dried-gel of the SPH-Im composite material was stripped from the Teflon® plate. The mixing ratio (*R*) of the Im was determined by equation (1):

$$R = \frac{[\text{Im}]}{[\text{Acidic amino acid in SPH}] + [\text{Im}]} \qquad (1)$$

where [Im] and [Acidic amino acid in SPH] are the molar concentration of Im and the molar concentration of the acidic amino acid, such as Glue and Asp, in the SPH, respectively. The amounts of the Glu and Asp in the SPH were determined by an amino acid analysis. The *R* value of the SPH-Im composite material was significantly changed from 0 to 1.

2.3. Characterization of composite materials.

The infrared (IR) spectra of the SPH-Im composite materials were characterized using an IR spectrophotometer FT/IR-4700 (JASCO Corporation, Tokyo, Japan) with the diamond attenuated total reflection (ATR) prism. The IR spectrum was measured with the resolution of 4 cm^{-1}. The thermal stabilities of the SPH-Im composite materials were analyzed using a DTG-60 thermogravimetric (TG) - differential thermal analyzer (DTA) (Shimadzu Corp., Kyoto, Japan). The TG-DTA measurement was performed at the heating rate of 10°C min^{-1} from room temperature to 300°C under flowing dry nitrogen. The sample weights of the TG-DTA measurements were normalized at 1 mg.

2.4. Proton conductivity measurements.

The proton conductivity of the SPH-Im composite material was measured by the a.c. impedance method in frequency range from 4 Hz to 1 MHz using a 35320-80 chemical impedance analyzer (Hioki

Co., Nagano, Japan) in a stainless vessel from room temperature to 130°C under dry flowing dry nitrogen. The composite membrane was sandwiched between two platinum electrodes (diameter: 6 mm) with the Teflon® spacer [19-21]. The thickness of the Teflon® spacer was 100 μm. The direction of the conductive measurement was perpendicular to the composite material. The conductivities of the composite materials were determined from a typical impedance response (Cole-Cole plots).

3. RESULTS AND DISCUSSION

3.1. Molecular structure of the SPH-Im composite material.

The protonated soy protein (SPH) and heterocyclic imidazole (Im) mixed solution was cast onto a Teflon® plate and dried. The dried-membrane or dried-gel of the SPH-Im was stripped from the Teflon® plate. At $R \leq 0.3$, the SPH-Im composite materials were produced in the membrane form. At $0.4 \leq R \leq 0.7$, the SPH-Im composite materials produced a gel-like form. In particular, at $0.6 \leq R$, the SPH-Im composite material indicated a liquid-like form with a low viscosity and these materials could not be used as a proton conductive sample. Furthermore, at $0.9 \leq R$, since the SPH-Im composite material contains a large amount of the Im molecule, these materials were in the powder form. Therefore, for the experiments, the SPH-Im composite materials, which were prepared at $0.1 \leq R \leq 0.5$, were used.

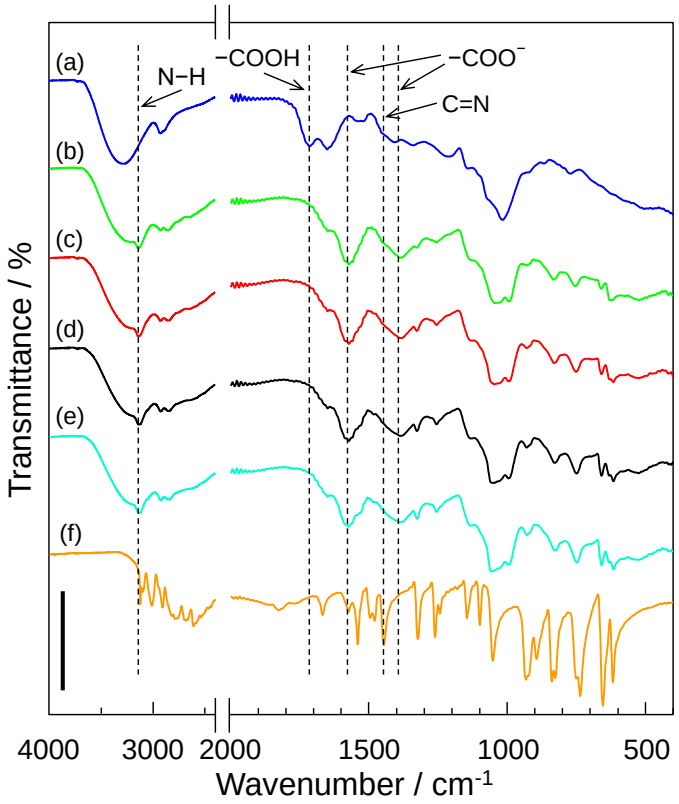

Figure 1. IR spectra of the SPH-Im composite materials with different Im mixing ratios. IR spectra were measured by the ATR method. (a) R=0 (pure SPH), (b) R=0.1, (c) R=0.2, (d) R=0.3, (e) R=0.5, and (f) the pure Im materials. These IR spectra were measured at the resolution of 4 cm^{-1}. Scale bar shows the transmittance of 50%. Triplicate experiments gave similar results.

The molecular structures of the SPH-Im composite material were characterized by infrared (IR) spectrometry using the ATR method. Figure 1 shows the IR spectra of (a) *R*=0 (pure SPH), (b) *R*=0.1, (c) *R*=0.2, (d) *R*=0.3, (e) *R*=0.5, and (5) the pure Im materials. The acidic amino acids, such as Glue and Asp, possess the –COOH group in their side chain [16]. Therefore, for the SPH material, the absorption band at 1715 cm^{-1}, attributed to the stretching vibration of C=O in –COOH [22,23], appeared (see spectrum (a) in Figure 1). This absorption band decreased with the increase in the *R* value (see spectra (b) – (e) in Figure 1). In addition, the absorption bands at 1572 cm^{-1} and 1385 cm^{-1}, related to the anti-symmetric and symmetric stretching vibrations of the $–COO^-$ [22,23], increased with the increase in the *R* value. As a result, the acidic –COOH group in the side chain of the SPH was deprotonated by the addition of the basic Im molecule. On the other hand, when the Im molecule was added to the SPH, the absorption band of the composite material at ca. 3200 cm^{-1}, a stretching vibration of the N–H group in the Im molecule [22-25], moderately increased in comparison to the intensity of the pure Im molecule. Additionally, the absorption band at 1446 cm^{-1}, the stretching vibration of C=N in the aromatic ring of the Im molecule [22], drastically decreased with the addition of the SPH. As a result, the basic –N= group in the aromatic ring of the Im molecule became protonated by the addition of the acidic SPH. These results suggested that the –COOH group in the side chain of the SPH produced the free proton by the mixing of the Im molecule and formed the $–COO^-$ group. The –N= group in the Im molecule by the mixing of the SPH accepted the free proton from the –COOH group and formed the –NH– group. Consequently, the SPH and Im produced the composite material through the acid-base interaction between the acidic –COOH and basic –N= groups. Similar phenomena have been reported for the acid-base composite material, such as the acidic polymer-heterocycle composite [14,18,23], nucleic acid-heterocycle composite [20], and polypeptide composite materials [26].

3.2. Thermal characteristic of the SP-Im composite material

The SPH and Im molecules formed the acid-base composite material through deprotonation of the –COOH group of acidic amino acid in the SPH and the protonation of the –N= group in Im by the mixing. Generally, the acid-base composite materials, which are prepared by mixing of acidic and basic molecules, are thermally stabilized by the acid-base interaction [14,18,23]. Therefore, the thermal stability of the SPH-Im composite material was measured by the thermogravimetric (TG) - differential thermal analyzer (DTA).

Figure 2 shows the TG (a) and DTA (b) curves of (1) *R*=0 (pure SPH), (2) *R*=0.1, (3) *R*=0.2, (4) *R*=0.3, (5) *R*=0.5, and (6) the pure Im materials. The TG-DTA measurements were done at the heating rate of 10°C min^{-1} from room temperature to 300°C under flowing dry nitrogen. At <100°C, the DTA curve of the pure SPH material showed a small endothermic peak, which is due to the evaporation of water from the SPH material. Additionally, the SPH material showed a moderate endothermic peak attributed to the thermal decomposition at 120 - 130°C. Therefore, at >130°C, the TG weight loss other than the evaporation of water appeared. In contrast, the Im molecule indicated two endothermic peaks at ca. 90°C and ca. 135°C, which are due to the melting and boiling of the Im molecule, respectively. These endothermic peaks disappeared by the mixing of the SPH. These phenomena, such as the

disappearance of endothermic peak by the addition of basic molecule, suggested that the Im molecules were thermally stabilized by the formation of the SPH-Im composite by the acid-base interaction. In fact, the endothermic peak of the SPH, which is related to the thermal decomposition, shifted to a higher temperature (see curves (3) – (5) in Figure 2(b)). Similar phenomena, such as the thermal stabilization through the acid-base interaction, have been reported for various composite materials [18,20,23,26]. These results suggested that the SPH-Im composite material can be used at ≤130°C. Therefore, we demonstrated the proton conductive measurements of the SPH-Im composite material under an anhydrous condition at ≤130°C.

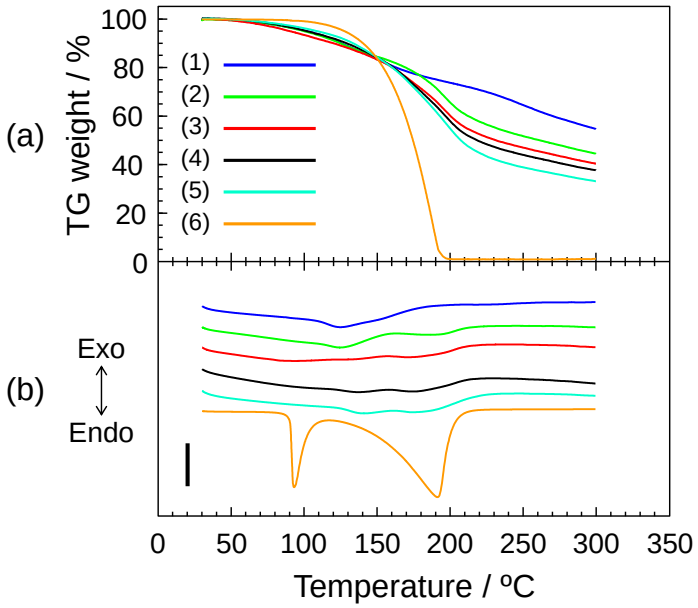

Figure 2. TG (a) and DTA (b) curves of the SPH-Im composite materials at the heating rate of 10°C min^{-1} under flowing dry nitrogen. (1) *R*=0 (pure SPH), (2) *R*=0.1, (3) *R*=0.2, (4) *R*=0.3, (5) *R*=0.5, and (6) the pure Im materials. The sample weights of the TG-DTA measurements were normalized at 1 mg. The scale bar in the DTA shows the heat quantity of 20 μV. Triplicate experiments gave similar results.

3.3. Proton conductivity of the SPH-Im composite material

The SPH-Im composite material in the stainless vessel was heated at 130°C for 2 hours under flowing dry nitrogen to evaporate the water and volatile components from the composite material. The composite materials were then cooled to room temperature under flowing dry nitrogen, and heated to measure the proton conductivity under flowing dry nitrogen once more. The proton conduction of the SPH-Im composite material was measured by the a.c. impedance method over the frequency range from 4 Hz to 1 MHz under the flowing dry nitrogen. The temperature range of the measurement was from room temperature to 130°C.

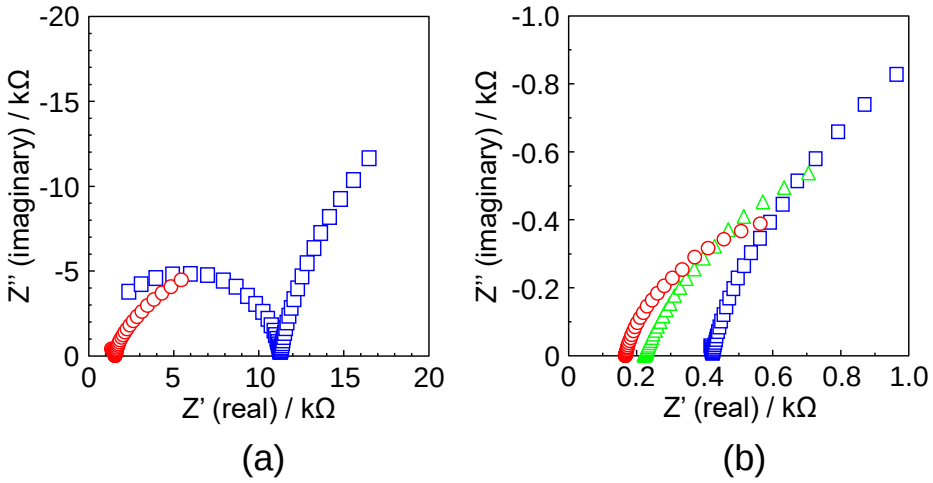

Figure 3. Typical impedance responses (Cole-Cole plot) of *R*=0.2 composite material at various temperatures. (a) (□) 60°C and (○) 80°C. (b) (□) 100°C, (△) 120°C and (○) 130°C. Frequency range (a) from 4 Hz to 1 MHz and (b) from 100 Hz to 1 MHz. Triplicate experiments gave similar results.

Generally, the typical impedance response (Cole-Cole plots) shows two semicircles in the high-frequency and low-frequency ranges [27]. The impedance responses at high-frequency and low-frequency are related to the conduction process in the bulk sample and at the electrode/solid electrolyte interface, respectively. For a highly proton conductive material, such as humidified Nafion® [11,28] and acidic polymer-heterocycle composite material [14,23] with high proton conductivity, the semicircle at the low-frequency decreases with the increase in the conductivity and disappears. Therefore, the bulk resistance of the sample is obtained by extrapolation to the real axis.

Figures 3 (a) and (b) show the Cole-Cole plots of *R*=0.2 composite material at 60 – 80°C and 100 – 130°C, respectively. The frequency ranges at (a) and (b) in Figure 3 were from 4 Hz to 1 MHz and from 100 Hz to 1 MHz, respectively. The semicircles at the high- and low-frequencies decreased with the increase in the temperature. The features of these responses at high temperature (100 – 130°C) are similar to that of highly proton-conducting materials, such as humidified Nafion® [11,28], acidic polymer-heterocycle composite material [14,23], and nucleic acid-heterocycle composite material [20]. Therefore, in this research, the bulk resistance of the SPH-Im composite material was calculated by extrapolation to the real axis based on previous reports [14,20,23]. On the other hand, the SPH-Im composite materials did not indicate an electronic conductivity under the DC condition. Additionally, the diffusible ions, such as alkaline metal ions, other than protons do not exist in the SPH-Im composite materials since the SPH materials have been purified by the ion exchange column. Furthermore, since the proton conductive samples have been heated at 130°C for 2 hours under flowing dry nitrogen and measured under flowing dry nitrogen, the SPH-Im composite materials do not contain water component. Therefore, the impedance responses during this measurement are due to the purely anhydrous proton conduction of the SPH-Im composite material.

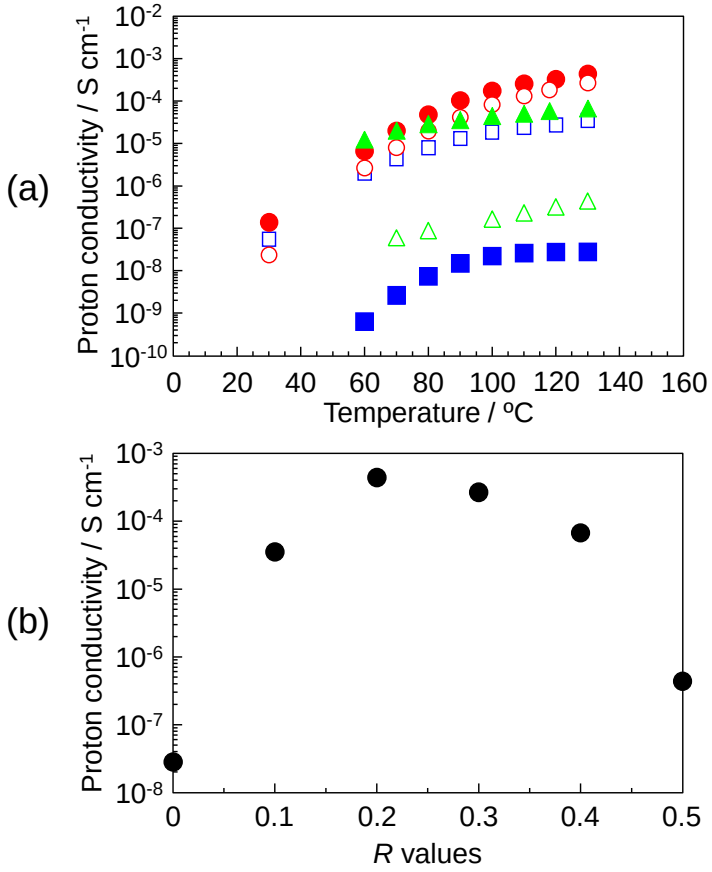

Figure 1. (a) Proton conductivities of the SPH-Im composite materials with different Im mixing ratios under anhydrous conditions. Mixing ratios of Im were (■) R=0 (pure SPH), (□) R=0.1, (●) R=0.2, (○) R=0.3, (▲) R=0.4, and (△) R=0.5 materials. (b) Change in the anhydrous proton conductivities of the SPH-Im composite materials at 130 °C as a function of the R values. Triplicate experiments gave similar results.

Figure 4 (a) shows the proton conductivities of the SPH-Im composite materials with different Im mixing ratios under flowing dry nitrogen. The mixing ratios of Im in Figure 4 (a) are (■) R=0 (pure SPH), (□) R=0.1, (●) R=0.2, (○) R=0.3, (▲) R=0.4, and (△) R=0.5 materials. The proton conductivity of the R=0 (SPH) material without mixing of the Im molecule was on the order of 10^{-10} S cm^{-1} at 60°C. This proton conductivity increased with the temperature and reached a maximum value on the order of 10^{-8} S cm^{-1} at 130°C. At > 130°C, the proton conductivity decreased by the thermal decomposition of the material (see TG-DTA in Figure 2). The proton conductivity of the composite materials when mixed with the Im molecule increased with the temperature and reached a maximum value at 130°C. Figure 4 (b) shows the proton conductivity of the SPH-Im composite material at 130 °C as a function of the R values. The proton conductivity at 130°C increased with the Im mixing ratio and reached a maximum value at R=0.2. This maximum proton conductivity at R=0.2 was 4.4×10^{-4} S cm^{-1}. At $0.3 \leq R$, the proton conductivity decreased and the conductivity at R=0.5 was on the order of 10^{-7} S cm^{-1}. On the other hand, for the SPH-Im composite material, which was prepared at $0.6 \leq R$, it could not be measured due to its liquid-like form. Additionally, the pure Im molecule without the mixing of the SPH material and the composite material at $0.9 \leq R$ could not demonstrate a proton conductive measurement due to melting

of the sample. These results suggested that the SPH-Im composite material becomes a proton conductor by the mixing of the basic materials.

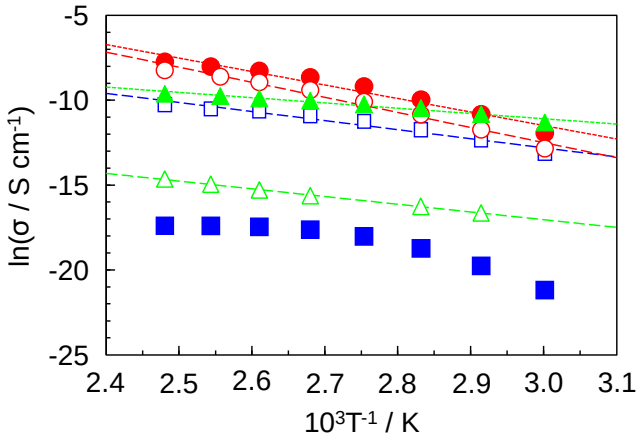

Figure 5. Arrhenius plots of the SPH-Im composite material. Solid lines are results of the least-squares fitting. Activation energies (E_a) of the proton transfer under anhydrous conditions were estimated from the slope of the linear line. Mixing ratios of Im were (■) R=0 (pure SPH), (□) R=0.1, (●) R=0.2, (○) R=0.3, (▲) R=0.4, and (△) R=0.5 materials. Triplicate experiments gave similar results.

Next, we estimated the proton conductive mechanism of the SPH-Im composite material from the activation energy (E_a) of the proton conduction. Figure 5 shows the Arrhenius plot of the proton conductivity of (■) R=0 (pure SPH), (□) R=0.1, (●) R=0.2, (○) R=0.3, (▲) R=0.4, and (△) R=0.5 materials. The solid lines in Figure 5 show the results of the least-squares fitting. Although the pure SPH material without the Im mixing could not fit a linear line, the composite materials showed linear lines at 60 – 130°C. These linear fittings suggested that the proton conductive mechanism of each composite material in these temperature ranges is an Arrhenius type behavior and single mechanism. Therefore, the E_a of the proton conduction in the SPH-Im composite material can be calculated from the slope of the linear line. Table 1 shows the E_a of the proton conduction in various SPH-Im composite materials. The estimated E_a values were 0.27 – 0.76 eV. The E_a of the SPH-Im composite material was more than one order of magnitude higher than that of humidified Nafion® [28] and almost the same as other anhydrous proton conductors, such as acid-base composite materials [14,20], solid electrolytes [29,30], and fullerene derivatives [31,32]. Therefore, the proton conduction of the SPH-Im composite material is ascribed to a non-vehicular mechanism in which only protons are mobile from the proton donor site to proton acceptor site without diffusible molecules [14,15]. The obtained E_a of the SPH-Im composite material relatively decreased with the increase of the R value. As a result, the E_a of the composite material showed two values, ca. 0.3 eV and ca. 0.7 eV. Especially, the E_a of ca. 0.3 eV with the high R value was the same as that of our reported anhydrous proton conductors [14,20,23].

Table 1. The activation energy (E_a) of proton conduction in the SPH-Im composite materials with various *R* values. The E_a values of the proton transfer under anhydrous conditions were estimated from the slope of the linear line in Figure 5.

Mixing ratio of Im	E_a / eV
R=0 (pure SPH)	−
R=0.1	0.46
R=0.2	0.68
R=0.3	0.76
R=0.4	0.27
R=0.5	0.39

−, Not determined

3.4. Proton conductive mechanism of the SPH-Im composite material

According to the E_a calculation, the proton conduction of the SPH-Im composite material was based on the non-vehicular mechanism without the assistance of diffusible molecules. In addition, the composite materials showed two E_a values, ca. 0.3 and ca. 0.7 (see Table 1). These results suggested that the composite materials have two proton conducting mechanisms by the different *R* values. These phenomena, such as the change of the proton conducting mechanism by the difference of *R* value, have been reported in various acid-base proton conductive materials [14,20]. The low E_a value, ca. 0.3 eV, was obtained with the high *R* value, in which Im molecules are relatively abundant in the composite material. In this case, the Im molecule accepts the free proton from the –COOH, related to the side chain of Glu and Asp, and forms the protonated Im (see IR spectra in Figure 1). Therefore, the proton transfer in the composite material occurs from the protonated Im to the non-protonated Im molecules. In other words, the protonated Im and the non-protonated Im molecules behave as a proton donor and proton acceptor in the SPH-Im composite material, respectively. In fact, the anhydrous proton conductor, which contains a large amount of Im, indicated a similar E_a value [14,20,23]. On the other hand, for the low *R* value, since the Im molecule is not abundant in the composite material, the proton transfer occurs in the protein. The –COOH group, attributed to the side chain of Glu and Asp, interacts with the basic Im molecule and forms the deprotonated $–COO^-$ group in the SPH-Im composite material (see IR spectra in Figure 1). Therefore, the proton transfer occurs from the –COOH group to the deprotonated $–COO^-$ group. In this case, the –COOH and the deprotonated $–COO^-$ groups in the composite material behave as a proton donor and proton acceptor, respectively. However, since the distance between the –COOH groups in the protein is long, the proton transfer does not easily occur in composite material. Therefore, the composite material with the low *R* value indicated a high E_a value, such as ca 0.7 eV. Similar high E_a values have been reported for the anhydrous acid-base proton conductor with the low heterocycle mixing ratio [14,20,23].

4. CONCLUSION

We prepared the SPH-Im composite material by the mixing of soy protein (SPH) and the imidazole (Im) molecule. This material formed an acid-base composite through the acid-base interaction between the acidic –COOH group, related to the side chain of acidic amino acids Glu and Asp, and basic Im molecule. In addition, the SPH-Im composite material showed a thermal stability at ≤130 °C. Furthermore, the SPH-Im composite material indicated the proton conductivity of 4.4×10^{-4} S cm^{-1} at 130 °C under flowing dry nitrogen. The E_a of the proton conduction was 0.27 – 0.76 eV. These E_a values were more than one order of magnitude higher than that of the proton conductive humidified Nafion® membrane. As a result, the proton conduction of the SPH-Im composite material behaves as a non-vehicular mechanism, in which only protons are mobile from the proton donor site to proton acceptor site without diffusible molecules. Therefore, the SPH-Im composite material may have potential applications not only for the PEFC operated under anhydrous or extremely low humidity conditions, but also for novel devices including bio- and chemical-sensors, bio-electrochromic materials, *etc*.

ACKNOWLEDGEMENTS
This work was supported by JSPS KAKENHI Grant Number JP19K12408, JP19K22298.

References

1. P.M. Visakh, O. Nazarenko, *Soy protein-based blends, composites and nanocomposites*, John Wiley & Sons, (1998) Hoboken.
2. H. El-Shemy, *Soybean bio-active compounds*, IntechOpen Limited, (2013) London.
3. C.M. Vaz, P.F.N.M. van Doeveren, R.L. Reis, A.M. Cunha, *Biomacromolecules*, 4 (2003) 1520.
4. C.M. Vaz, M. Fossen, R.F. van Tuil, L.A. de Graaf, R.L. Reis, A.M. Cunha, *J. Biomed. Mater. Res. A.*, 65 (2003) 60.
5. S. Rani, R. Kumar, *J. Polym. Environ.*, 27 (2019) 1613.
6. M. Yamada, S. Morimitsu, E. Hosono, T. Yamada, *Int. J. Biol. Macromol.*, 149 (2020) 1077.
7. C. Klockenbusch, J.E. O'Hara, J. Kast, *Anal. Bioanal. Chem.*, 404 (2012) 1057.
8. H. Gao, K. Lian, *RSC Adv.*, 4 (2014) 33091.
9. E. Quartarone, S. Angioni, P. Mustarelli, *Materials*, 10 (2017) 687.
10. L. Cao, X. He, Z. Jiang, X. Li, Y. Li, Y. Ren, L. Yang, H. Wu, *Chem. Soc. Rev.*, 46 (2017) 6725.
11. Y. Sone, P. Ekdunge, D. Simonsson, *J. Electrochem. Soc.* 143 (1996) 1254-1259.
12. K.D. Kreuer, *Chem. Mater.*, 8 (1996) 610.
13. K.D. Kreuer, *Chem. Mater.*, 26 (2014) 361.
14. I. Honma, M. Yamada, *Bull. Chem. Soc. Jpn.*, 80 (2007) 2110.
15. J.A. Asensio, E.M. Sánchez, P. Gómez-Romero, *Chem. Soc. Rev.*, 39 (2010) 3210.
16. J. Crowe, T. Bradshaw, P. Monk, *Chemistry for the biosciences*, Oxford University Press, (2006) New York.
17. W. Saenger, *Principles of Nucleic Acid Structure*, Springer-Verlag, (1987) Berlin.
18. M. Yamada, M. Takeda, *Int. J. Electrochem. Sci.*, 13 (2018) 7291.
19. M. Suzuki, T. Yoshida, S. Kobayashi, T. Koyama, M. Kimura, K. Hanabusa, H. Shirai, *Phys. Chem. Chem. Phys.*, 1 (1999) 2749.
20. M. Yamada, A. Goto, *Polymer J.*, 44 (2012) 415.
21. C. Tiyapiboonchaiya, J.M. Pringle, J. Sun, N. Byrne, P.C. Howlett, D.R. MacFarlane, M. Forsyth,

Nat. Mater., 3 (2004) 29.
22. R.M. Silverstein, F.X. Webster, *Spectrometric Identification of Organic Compounds*, John Wiley & Sons, (1998) New York.
23. M. Yamada, I. Honma, *Polymer*, 45 (2004) 8349.
24. A. Bozkurt, W.H. Meyer, *Solid State Ionics*, 138 (2001) 259.
25. A. Bozkurt, W.H. Meyer, J. Gutmann, G. Wegner, *Solid State Ionics*, 164 (2003) 169.
26. M. Yamada, Y. Moritani, *Electrochim. Acta*, 144 (2014) 168.
27. M.A. Vargas, R.A. Vargas, B.E. Mellander, *Electrochim. Acta*, 44 (1999) 4227.
28. C.K. Subramaniam, C.S. Ramya, K. Ramya, *J. Appl .Electrochem.*, 41 (2011) 197.
29. P. Colomban, A. Novak, *J. Mol. Struct.*, 177 (1988) 277.
30. H. Iwahara, *Solid State Ionics*, 86-88 (1996) 9.
31. K. Hinokuma, M. Ata, *Chem. Phys. Lett.*, 341 (2001) 442.
32. Y.M. Li, K. Hinokuma, *Solid State Ionics*, 150 (2002) 309.